Cellulose
DOI 10.1007/s10570-014-0303-6

ORIGINAL PAPER

Comparison of changes in cellulose ultrastructure during different pretreatments of poplar

Qining Sun · Marcus Foston · Daisuke Sawada · Sai Venkatesh Pingali · Hugh M. O'Neill · Hongjia Li · Charles E. Wyman · Paul Langan · Yunqiao Pu · Art J. Ragauskas

Received: 11 November 2013 / Accepted: 14 May 2014

Abstract One commonly cited factor that contributes to the recalcitrance of biomass is cellulose crystallinity. The present study aims to establish the effect of several pretreatment technologies on cellulose crystallinity, crystalline allomorph distribution, and cellulose ultrastructure. The observed changes in the cellulose ultrastructure of poplar were also related to changes in enzymatic hydrolysis, a measure of biomass recalcitrance. Hot-water, organo-solv, lime, lime-oxidant, dilute acid, and dilute acid-oxidant pretreatments were compared in terms of changes in enzymatic sugar release and then changes in cellulose ultrastructure measured by ^{13}C cross polarization magic angle spinning nuclear magnetic resonance and wide-angle X-ray diffraction. Pretreatment severity and relative chemical depolymerization/degradation were assessed through compositional analysis and high-performance anion-exchange chromatography with pulsed amperometric detection. Results showed minimal cellulose ultrastructural changes occurred due to lime and lime-oxidant pretreatments, which at short residence time displayed relatively high enzymatic glucose yield. Hot water pretreatment moderately changed cellulose crystallinity and crystalline allomorph distribution, yet produced the lowest enzymatic glucose yield. Dilute acid and dilute acid-oxidant pretreatments resulted in the largest increase in cellulose crystallinity, *para*-crystalline, and cellulose-I_β allomorph content as well as the largest increase in cellulose microfibril or crystallite size. Perhaps related, compositional analysis and Klason lignin contents for samples that underwent dilute acid and dilute acid-oxidant pretreatments indicated the most significant polysaccharide depolymerization/degradation also ensued. Organo-solv pretreatment generated the highest glucose yield, which was accompanied by the most significant increase in cellulose microfibril or crystallite size and decrease in relatively lignin contents. Hot-water, dilute acid, dilute acid-oxidant, and organo-solv pretreatments all showed evidence of cellulose microfibril coalescence.

Q. Sun · Y. Pu · A. J. Ragauskas (✉)
School of Chemistry and Biochemistry, Institute of Paper Science and Technology, Georgia Institute of Technology, 500 10th St., Atlanta, GA 30332, USA
e-mail: art.ragauskas@chemistry.gatech.edu

M. Foston
Department of Energy, Environmental and Chemical Engineering, Washington University, 1 Brookings Drive, Saint Louis, MO 63130, USA

D. Sawada · S. V. Pingali · H. M. O'Neill · P. Langan
Center for Structural Molecular Biology, Biology and Soft Matter Division, Oak Ridge National Laboratory, Oak Ridge, TN 37831, USA

H. Li · C. E. Wyman
BioEnergy Science Center, Center for Environmental Research and Technology, Chemical and Environmental Engineering Department, Bourns College of Engineering, University of California, Riverside, CA 92507, USA

Published online: 24 May 2014

Keywords Biomass pretreatment · Cellulose · Ultrastructure · Crystallinity · Enzymatic hydrolysis

Introduction

Several *Populus* species are presently being developed as high potential energy crops because they exhibit drought tolerance, pests and insects resistance, and high biomass yields on a range of lands (Sannigrahi et al. 2010c). More importantly, through genetic modification, the extensive sequencing of the *Populus* genome has made it possible to enhance many of these characteristics unlike ever before (Brunner et al. 2004). Potential applications for poplar include biofuels, pulp and paper, a variety of wood-based products, and the next generation of commodity and fine chemicals. Among the most promising utilization of poplar feedstocks is the production of bioethanol (Sannigrahi et al. 2010c). Considering the inherent resistant of lignocellulosic cell walls to deconstruction by microbes and enzymes (i.e., biomass recalcitrance), current cellulosic bioethanol production requires pretreatment prior to enzymatic hydrolysis and fermentation. The goal of this pretreatment has commonly been cited as a process to (1) open the lignin-hemicellulose matrix, (2) alter and re-distribute structural components in the cell wall, (3) lower the degree of polymerization of cellulose, and (4) disrupt the ultrastructure of the cellulose, ultimately aimed at enhancing substrate accessibility and digestibility for enzymatic hydrolysis (Mosier et al. 2005b).

Pretreatment of lignocellulosic materials can include physical, physicochemical, chemical, and biological processes, of which chemical pretreatments typically utilize acid or base with controlled time, temperature, and pH profiles and/or organic solvents to facilitate cell wall component removal (Chang et al. 2001; Brosse et al. 2009; Hu and Ragauskas 2012). One of the most promising options because of cost effectiveness and ease of scalability employs dilute sulfuric acid (0.5–1.0 %) at moderate temperatures (140–190 °C) to hydrolyze hemicelluloses, disrupt lignin and enhance sugar yield in subsequent enzymatic deconstruction of cellulose (Lloyd and Wyman 2005; Foston and Ragauskas 2010).

Kumar et al. (2009) conducted a comprehensive study applying some of the leading pretreatment technologies including ammonia fiber expansion, aqueous ammonia recycle, dilute sulfuric acid, lime, neutral pH, and sulfur dioxide to poplar, evaluating each technology based on enzymatic release following a common sugar assay procedure. This particular study indicated that one of the most notable changes in the composition of dilute acid pretreated solids is a significant reduction in the relative hemicellulose content. Wyman et al. (2009) showed that dilute acid pretreatments of poplar facilitated ethanol yields of approximately 85 % when using simultaneous saccharification and fermentation (SSF), and produced glucose yields around 64 % when using separate hydrolysis and fermentation (SHF).

Another very common treatment is hot water pretreatment (i.e., without adding acid or base) referred to as auto-hydrolysis because the hot water cleaves acetyl and hemiacetal linkages, liberating acids along with the natural acidity of water catalyzes the hydrolysis of linkages in the cell wall. This pretreatment is associated with lower capital and production costs and reduced formation of degradation products (Mosier et al. 2005a).

An alternative to acidic pretreatments are alkali pretreatments which are processes that typically utilize lower temperatures and pressures when compared to other pretreatment technologies. The commercial application of alkaline bases is often not preferred because sodium hydroxide and other bases are costly and difficult to recover and to reuse in a cost-effective manner (Mosier et al. 2005b). Lime pretreatment with proven effectiveness and low cost (Chang et al. 1998) has been used to pretreat a variety of substrates including poplar. Wyman et al. (2009) demonstrated lime pretreatment of poplar exhibited a reduction in relative lignin content rather than hemicelluloses with SHF glucose yields of ~71 %. Chang et al. (1997) conducted a systematic study of lime pretreatment conditions on switchgrass and found a residence time of 2.0 h at 100–120 °C with a 0.1 g $Ca(OH)_2$/g dry biomass lime loading and water loading of 9 mL/g of dry biomass as optimal to enhance enzymatic digestibility.

An additional interesting class of pretreatment technologies includes wet oxidant methods (Martin et al. 2007). For example, lime and oxygen were used to enhance the enzymatic digestibility of poplar in a

study by Chang et al. (2001) indicating a partial pressure of 1.4 MPa of absolute oxygen gave the optimal condition to enhance the enzymatic digestibility, with a 3 days total enzymatic sugar conversion of ~97 %.

Understanding the structural parameters relevant to plant cell wall recalcitrance and how those parameters individually and cooperatively affect enzymatic saccharification are vital for improving current processing and conversion methods for cellulosic biofuels. Though, in more recent work, research has started to indicate that increases in accessibility may be one of the major first order rate determining factors in enzymatic hydrolysis (Mosier et al. 2005b; Meng et al. 2013). However, among various substrate characteristics cellulose morphology and crystallinity index are inherently connected with cellulase enzyme activity and therefore efficient enzymatic hydrolysis of lignocelluloses (Bubner et al. 2013; Foston and Ragauskas 2012; Zhao et al. 2006). A study by Pu et al. (2006) examined the enzymatic hydrolysis of bleached softwood Kraft pulps in which they reported a faster decrease in the relative amount of amorphous cellulose as a function of enzymatic hydrolysis time. Recent research studies on the structural reorganization of cellulose fibrils during hydrothermal deconstruction and their relationship with enzymatic digestion indicated that cellulose morphological changes occurred within the lignocellulosic cell wall as a result of pretreatment deconstruction and that these changes are very important for maximizing enzyme digestibility and minimizing energy consumption (Ibbett et al. 2013). This suggests cellulose ultrastructure is a substrate characteristic relevant to the enzymatic deconstruction of biomass and must be monitored to not only deconvolute the factors affecting recalcitrance but also to help develop a deeper understanding of the molecular-level mechanisms that these enzymes employ. A vital component of this is to generate reliable structural models of cellulose before and after pretreatment. These results can be then used in further research such as computational methods applied model to cell wall deconstruction or the generation of new optimized biocatalysts and low-recalcitrant genetically engineered plants.

In this study, a *Populus trichocarpa x deltoides* hybrid was subjected to hot-water, organo-solv, lime, lime-oxidant (lime/Ox), dilute acid and dilute acid-oxidant (dilute acid/Ox) pretreatments. These samples were then examined for changes in cellulose ultrastructure during pretreatment by ^{13}C cross polarization magic angle spinning (CP/MAS) nuclear magnetic resonance (NMR) and wide-angle X-ray diffraction (WAXD). An enzymatic recalcitrance screen was performed to evaluate and compare the changes in glucose sugar release with respect to different types of pretreatment. Moreover, in this study we intended to investigate transformations occurring in cellulose ultrastructure during various pretreatments, and examine possible links between changes in sugar release (i.e., biomass recalcitrance) and alterations in cellulose crystallinity and crystalline allomorph distribution.

Materials and methods

Substrates

Baseline poplar (*Populus trichocarpa x deltoides*) samples were harvested between 2007 and 2008 by National Renewable Energy Laboratory (NREL) at area 0800 at Oak Ridge National Laboratory, TN. The biomass was size-reduced in a Wiley mill using a 0.250–0.177 mm screen. Extractives were subsequently removed by placing the biomass into an extraction thimble in a Soxhlet extraction apparatus. The extraction flask was filled with 1:2 ethanol/benzene mixture (~150 mL) and then refluxed at a boiling rate which cycled the biomass for at least 24 extractions over a 4 h period.

Pretreatments

The lignocellulosic material was transferred to a 4560 mini-Parr 300 ml pressure reactor with a pretreating solution prepared as described in Table 1 at 5.0 % dry solids and then sealed. The impeller speed was set to about 100 rpm, and the vessel was heated to a temperature as described in Table 1 over ~25–30 min (at ~6 °C/min). The reactor was held at the pretreatment temperature ±2 °C (120–160 °C; ~0.65–0.69 MPa) for the specified residence time ± 30 s. The reactor was then quenched in an ice bath (~5 min). Pretreatment conditions were adapted from literature which investigated optimal pretreatment conditions (Chang et al. 1997; Kumar et al. 2009; Wyman et al. 2009). The pretreated slurry was filtered to remove the solid material and washed with an excess of deionized (DI)

Table 1 Various pretreatments conducted on hybrid poplar

Pretreatment	Reagents	Pretreatment residence time (min)	Temp (°C)	% dry solids
Hot water	H_2O	5, 10, 60	160	5
Dilute acid	0.1 M H_2SO_4	5, 10, 60	160	5
Dilute Acid/Ox	0.1 M H_2SO_4, 0.55 MPa of O_2	5, 10, 60	160	5
Organo-solv	0.02 M H_2SO_4, 65 % ethanol/water	5, 10, 60	160	5
Lime	0.1 M $Ca(OH)_2$	5, 10, 60	120	5
Lime/Ox	0.1 M $Ca(OH)_2$, 0.55 MPa of O_2	5, 10, 60	120	5

filtered water. Paramagnetic impurities were removed by washing the solids with a 2 % aqueous solution of ethylenediaminetetraacetic acid (EDTA) and DI water. The pretreated lignocellulosic samples were then dried in the fume hood overnight. All gravimetric yields for biomass recovered after pretreatment ranged between 75–85 %.

Carbohydrates and Klason lignin analysis

In order to monitor biomass composition change as a result of pretreatments and calculate the sugar conversion from enzymatic hydrolysis, carbohydrate and Klason lignin analysis were carried out based on methods described in Tappi T-249 (Davis 1998). The first stage utilized a high concentration acid and a low reaction temperature (72 vol% H_2SO_4 at 30 °C for 1 h). The second stage was performed at much lower acid concentration and higher temperature (3 vol% H_2SO_4 at 121 °C for 1 h) in an autoclave. The resulting solution was cooled to room temperature and filtered using G8 glass fiber filter (Fisher Scientific, USA). The remaining residue is considered as Klason lignin which was oven-dried and weighed to obtain the Klason lignin content. The filtered solution was analyzed for carbohydrate constituents of the hydrolyzed poplar samples determined by high-performance anion-exchange chromatography with pulsed amperometric detection (HPAEC-PAD) using Dionex ICS-3000 (Dionex Corp., USA). Error analysis was conducted by performing carbohydrate and Klason lignin analysis three times on the untreated and pretreated lignocellulosics.

Sample preparation for NMR

In order to compare cellulose ultrastructural changes during various pretreatments, cellulose from various pretreated poplar samples was isolated and purified for NMR analysis. Holocellulose was first isolated from pretreated poplar samples by treatment with $NaClO_2$ (1.30 g/1.00 g lignocellulosic dry solids) in acetic acid (375.00 mL of 0.14 M) at 70 °C for 2 h. The samples were then collected by filtration and rinsed with an excess of DI water. Isolated cellulose was prepared from the holocellulose sample (1.00 g) by refluxing with HCl (100.0 mL of 2.50 M) as reported by Foston (2010). The isolated cellulose samples were then collected by filtration and rinsed with an excess of DI filtered water, and air dried. Illustration of the procedure is shown in Fig. 1.

NMR analysis of cellulose

The cellulose samples with ~55 % water content were prepared with isolated cellulose packed into a 4-mm cylindrical ceramic MAS rotor. Repetitive steps of packing sample into the rotor were performed to fully compress and load the maximum amount of sample. Solid-state NMR measurements were carried out on a Bruker DSX-400 spectrometer operating at frequencies of 100.55 MHz for ^{13}C in a Bruker double-resonance MAS probehead at spinning speeds of 10 kHz. CP/MAS experiments utilized a 5 μs (90°) proton pulse, 1.5 ms contact pulse, 4 s recycle delay and 4–8 K scans. All spectra were recorded on wet samples, and the line-fitting analysis of spectra was performed using NUTS NMR Data Processing software (Acorn NMR, Inc) as reported by Foston (2009, 2010). Error analysis was conducted by performing three individual isolations, NMR acquisitions and line-fit data processing.

WAXD analysis of untreated and pretreated poplar

WAXD measurements were performed using a theta–theta goniometer PANalytical X'Pert PRO diffractometer with Cu $K\alpha$ radiation ($\lambda = 1.542$ Å) operating

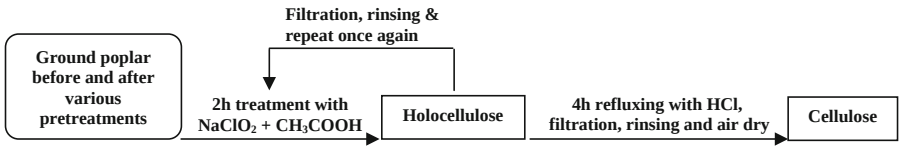

Fig. 1 Illustration of cellulose sample preparation for NMR test

at 45 kV and 40 mA. Beam divergence on the incident and diffracted beam paths are controlled by the programmable divergence and programmable anti-scatter slits to maintain a constant illuminated spot of 10 mm on the sample. A fixed 2° anti-scatter slit and a 10 mm width limiting beam mask on the incident beam path; soller slits of 0.04 rad divergence on both beam paths; Nickel as a beta-filter and X'Celerator scientific detector on the diffracted beam path were the other optic components. The pretreated poplar samples, covered with a kapton film to maintain its humidity during measurements, were mounted onto the Spinner PW3064 stage and rotated at 7.5 rpm. Data was collected in the continuous scan mode from 5° to 90° 2θ. The width of the diffraction peaks associated with specific reflecting planes (*hkl*) having a repeat spacing of d_{hkl} was used to estimate the crystallite size, L_{hkl} using the Scherrer equation.

The crystallite size (or dimension) L_{hkl} is calculated by the relation (Cullity and Stock 2001; Klug and Alexander 1974; Park et al. 2010):

$$L_{hkl} = \frac{0.9\lambda}{\beta_{hkl} \cos\,\theta} \tag{1}$$

where λ is the X-ray wavelength in Å; is the angular full-width at half maximum intensity (FWHM) in radians of the (*hkl*) line profile; and θ is the scattering angle. The calculated values of crystallite size, L_{200} were obtained from diffraction peak widths according to the Scherrer method for all samples.

Down-scaled enzymatic sugar release assay

The sugar release values were determined based on the High Throughput Pretreatment and Enzymatic hydrolysis (HTPH) designed at University of California, Riverside (Studer et al. 2010). In this study, 4.5 mg dry biomass was loaded into individual wells of a custom-built metal well plate by an automation robotics platform (Symyx Technologies, Sunnyvale, CA). Then, 446 µL deionized (DI) water was pipetted into all wells (8 channel pipette, 30–300 µL, Eppendorf, Hamburg, Germany) to achieve a solid loading of 1 wt%. Next, 39 µL of a mixture of 1 M citrate buffer (pH 4.8), sodium azide solution and enzymes was pipetted into each well (8 channel pipette, 10–100 µL, Eppendorf, Hamburg, Germany). The final hydrolyzates contained 0.05 M citrate buffer (pH 4.95), and 0.2 g/L sodium azide. The resulting enzyme loading corresponded to 112.5 mg of Accellerase 1500 and 37.5 mg of Accellerase XY protein (Genencor, Palo Alto, CA, USA), respectively, per g of glucan + xylan in tested biomass. After enzyme addition, the well plate was then clamped between two stainless steel plates with a flat silicone gasket in between. The plate was then placed on its side in an incubation shaker (Multitron Infors-HT, ATR Biotech, Laurel, MD, USA) at 50 °C for 72 h at 150 rpm. Following enzymatic hydrolysis, the well plate block was allowed to cool to room temperature and then opened. A sealing tape (Nunc, Rochester, NY) was secured to the top of all vials and the entire well plate was centrifuged (CS-6R Centrifuge, Beckman, Fullerton, CA) for 20 min at 2,650 rpm. Then, 260 µL of the clear hydrolyzates solution was transferred to a PP 96-well plate (Agilent, Santa Clara, CA, USA) for HPLC analysis. In this part, sugar concentrations were quantified using Agilent 1200 HPLC (Agilent, Santa Clara, CA, USA) equipped with an Aminex HPX-87H column (BioRad, Hercules, CA, USA) and a refractive index detector.

Results and discussion

Cell wall composition

Carbohydrate and Klason lignin values for the different pretreatments as described in Table 1 are reported in Fig. 2 for untreated and pretreated solids. Alkaline pretreatments, lime and lime/Ox, did not significantly alter the relative carbohydrate and Klason lignin

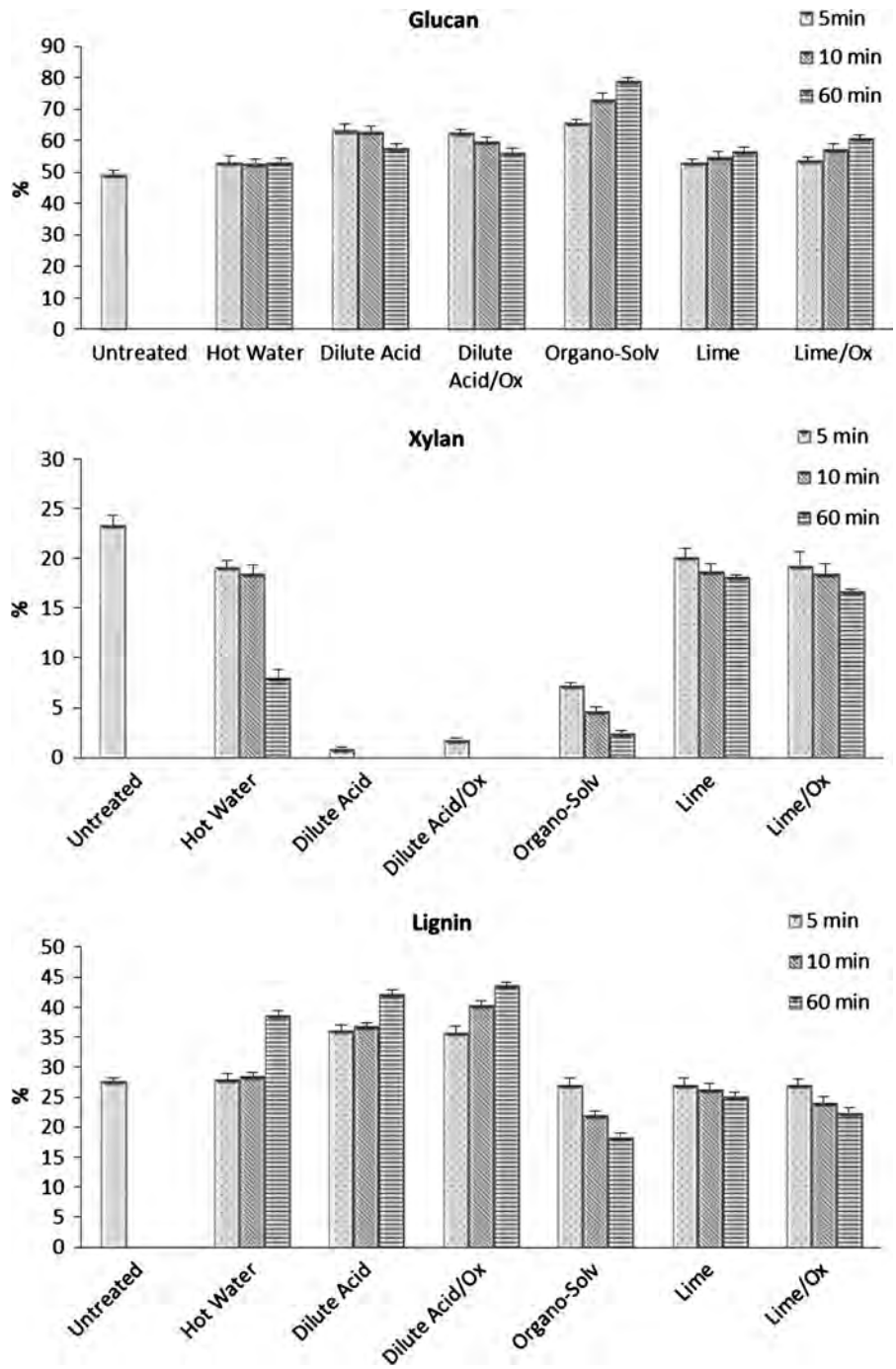

Fig. 2 Relative glucan, xylan and lignin contents in the residual untreated and pretreated poplar solids

distributions, which is in agreement with previous studies under the similar experimental conditions (Xu et al. 2010; Xu and Cheng 2011; Wang and Cheng 2011). These studies suggested little alteration in the compositional analysis of alkaline pretreated biomass occurred, in part, due to the relatively lower pretreatment temperatures utilized. In this case compositional analysis indicated lime and lime/Ox pretreatment were much less severe than the other pretreatments conducted and would consequently cause less alterations

and degradation to the remaining cellulosic components. On the other hand, dilute acid and dilute acid/Ox pretreatments removed the most significant fraction of xylan, increasing the relative Klason lignin content by almost 50 %. This accompanying increase in the relative Klason lignin content observed for acid pretreatments could be attributed to not only the hydrolysis of hemicellulose and maybe cellulose but also the formation of 'pseudo-lignin', a polysaccharide degradation product resulting from the repolymerization of dehydrated sugars forming lignin-like polyphenolic structures (Sannigrahi et al. 2011). The fact cellulosic components may have been degraded/removed during acid pretreatments that could have large implication on concurrent changes in cellulose ultrastructure. Organo-solv pretreatment reduced the relative Klason lignin content significantly (by ~33 %) while removed most of the xylan and yielded a glucan rich solid component. Lignin content reduction in organo-solv pretreatment could result from solubilization and fragmentation that release lignin into the organic phase (Pan et al. 2008; Sannigrahi et al. 2010b). Though only reporting relative change in cell wall composition, compositional analysis seems to suggest organo-solv pretreatments may also degrade/remove cellulose. Similarly, hot water pretreatment after a 60 min residence time appears chemically comparable to biomass that underwent dilute acid pretreatment, partially removing xylan and increasing the relative Klason lignin content.

Cellulose crystallinity and ultrastructure analysis by NMR

The direct polarization magic-angle spinning (DP/MAS) experiments with a long enough recycle delay permits complete T_1 relaxation of the observed nuclei and can provide the most reliable method for obtaining quantitative solid state NMR spectra; however, it is usually time-consuming to aquire an acceptable signal-to-noise ratio. Compared to DP/MAS, CP/MAS can enhance the signal intensity per measuring time by about an order of magnitude. While the difference in magnetization transfer from ^{1}H to carbons bonded to ^{1}H and to nonprotonated ^{13}C or mobile segments with weaker ^{1}H–^{13}C dipolar couplings can make quantification of CP/MAS spectra difficult, quantitation can be achieved with

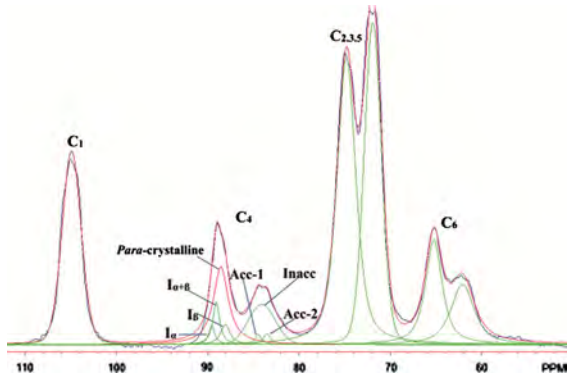

Fig. 3 Non-linear least-squared line fitting of the C_4 region of ^{13}C NMR spectrum of isolated cellulose samples

carefully choosen experimental conditions. The quantitative analysis of the particular cellulose C_4-peak at the selected chemical shift has been documented in literature with the choice of the optimal contact time and applied experimental conditions that maximizes the signal intensity (Pu et al. 2006; Foston and Ragauskas 2010).

The cellulose C_4-carbon region extends over a ^{13}C NMR chemical shift range of δ ~80–93 ppm as shown in Fig. 3. A commonly used probe for cellulose amorphous domains can be observed at a ^{13}C chemical shift range of δ ~80–85 ppm, appearing as a series of fairly broad and overlapping resonances. ^{13}C CP/MAS NMR spectroscopy experiments were conducted to determine cellulose % crystallinity as shown in Fig. 4. Cellulose % crystallinity is calculated by dividing the area of the crystalline peak by the total area assigned to the C_4-carbon region.

The non-linear least-squared line fitting of the C_4-region for a ^{13}C CP/MAS spectra of isolated cellulose prepared from pretreated poplar are presented in Fig. 3. The deconvolution was performed by fitting seven lines to the C_4 region with additional constraints for the areas of the three Lorentzian lines that originate from crystalline cellulose allomorphs I_α (90.2–89.7 ppm), I_β (88.1–87.8 ppm) and $I_{\alpha+\beta}$ (89.0–88.6 ppm), and four Gaussian lines for non-crystalline cellulose accessible fibril surfaces (Acc-1: 84.9–84.2 and Acc-2: 83.6–83.2 ppm) and inaccessible fibril surface (Inacc: 83.9–83.4 ppm) as well as *para*-crystalline cellulose (88.6–88.4 ppm) (VanderHart and Atalla 1984; Maciel et al. 1982; Wickholm et al. 1998; Sannigrahi et al. 2010a; Foston and Ragauskas 2010). The relative intensity of the cellulosic ultrastructural components

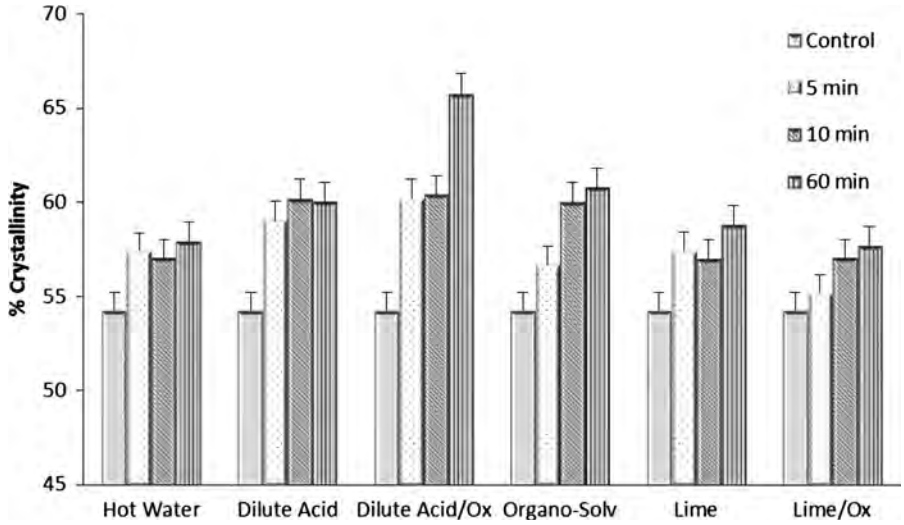

Fig. 4 % Crystallinity of cellulose in the residual pretreated hybrid poplar solids as determined by acid isolated cellulose and ^{13}C CP/MAS NMR spectra

Table 2 The relative % cellulose crystalline allomorphs, *para*-crystalline cellulose and cellulose fibril surface in the residual hybrid poplar solids pretreated for 60 min

Treatments	I_α ±0.3 (%)	$I_{\alpha+\beta}$ ±0.3 (%)	Para ±1.5 (%)	I_β ±0.3 (%)	Inacc ± 1.6 (%)	Acc-1 ±0.3 (%)	Acc-2 ±0.3 (%)	LFD ±0.2 (nm)	LFAD ±3.0 (nm)
Untreated	4.0	8.6	37.5	4.2	39.4	4.2	2.1	4.2	34
Hot water	3.1	7.5	40.5	6.9	37.4	2.9	1.7	4.6	47
Dilute acid	3.6	5.7	43.0	7.8	35.8	2.5	1.7	4.9	52
Dilute acid/Ox	1.7	8.9	45.9	9.3	30.3	3.3	0.6	5.8	55
Organo-solv	3.6	6.0	44.8	6.4	35.5	2.1	1.6	5.0	59
Lime	2.6	7.9	40.7	7.7	35.1	3.4	2.6	4.7	36
Lime/Ox	3.1	4.6	45.1	4.9	37.0	3.1	2.2	4.6	41

Para para-crystalline cellulose, *Inacc* inaccessible fibril surface, *Acc-1 and Acc-2* accessible fibril surface, *LFD* lateral fibril dimension, *LFAD* lateral fibril aggregate dimension

within cellulose fibrils and how those relative intensities change with pretreatment at the most severe conditions tested are shown in Table 2. In addition, the percentage of C_4-carbons detected at fibril surfaces and along a square cross-sectional cellulose microfibril model, can be used to estimate the cellulose microfibril [i.e., lateral fibril dimension (LFD) or cellulose crystallite dimension] and microfibril bundle [i.e., lateral fibril aggregate dimension (LFAD)] dimensions.

The generalized major effects of the pretreatments on cellulose ultrastructure are: (1) increases in cellulose % crystallinity, (2) increases in the relative cellulose I_β and *para*-crystalline content, (3) increases in cellulose LFD and LFAD, and (4) decreases in the relative cellulose I_α content, cellulose accessible fibril surfaces, and cellulose inaccessible fibril surfaces. The observed increase in relative cellulose I_β content is accompanied by a reduction in resonances representing cellulose $I_{\alpha+\beta}$ and I_α content. This change most likely results from the thermal transformation of the cellulose I_α allomorph, which has a meta-stable triclinic one-chain crystal structure, to the cellulose I_β allomorph, a more thermodynamic favored monoclinic two-chain crystal structure (Debzi et al. 1991; Foston and Ragauskas 2010). Moreover, pretreatments resulted in the increase of *para*-crystalline

cellulose content and a concurrent decrease in the relative proportion of amorphous (i.e., accessible and inaccessible fibril surfaces) cellulose. In conjunction with compositional analysis suggesting cellulosic degradation occurs and a previous study indicating hydrolysis of amorphous cellulose is kinetically favored over that of crystalline cellulose (Pu et al. 2006), increases in % crystallinity and even perhaps relative *para*-crystalline cellulose content could result from the preferential degradation/removal of amorphous cellulose during pretreatment (Foston and Ragauskas 2010; Samuel et al. 2010).

Various pretreatments increased cellulose % crystallinity to different extents. Acidic pretreatments increased the crystallinity significantly, while alkaline pretreatments including lime and lime/Ox had relatively less effect. This aligns with compositional analysis indicating amorphous cellulose is more susceptible to hydrolysis at acidic pretreatment conditions than at alkaline pretreatment conditions. The increase of cellulose % crystallinity in pretreated poplar could result from a combination of several factors. Aside from preferential removal of amorphous cellulose (see Table 2), a hydrothermal "annealing"-like process that transforms cellulose I_{α} into cellulose I_{β} could also lead to ordering of amorphous cellulose into *para*-crystalline cellulose (Sturcova et al. 2004).

Hornification describes the irreversible stiffening and shrinking of lignocellulosic materials upon drying or water removal. Hornification shrinks internal fiber volume, and upon re-suspension in water the original extent of water-swelling is not obtained. Interestingly, hornification is not only associated with decreases in water retention value, specific surface area, and pore size (Diniz et al. 2004) but also with accompanying increases in crystallinity and crystallite size (Chen et al. 2010; Newman 2004). Several mechanisms have been proposed to explain hornification in lignocellulosic materials (Ostlund et al. 2010; Foston and Ragauskas 2010). One such proposed mechanism, co-crystallization of adjacent cellulose microfibrils (Oksanen et al. 1997; Newman 2004), may also be used here to explain the observed cellulose % crystallinity increases occurring as a result of severe pretreatment. However, if co-crystallization is indeed occurring, cellulose crystallite dimensions might be expected to increase as well.

Based on the LFD and LFAD results (see Table 2), cellulose isolated from acid, acid/Ox, and organo-solv pretreated poplar displayed significant increases in LFD and LFAD as compared to cellulose isolated from hot water, lime, and lime/Ox pretreated poplar. Previous pretreatment studies have attributed this increase in LFD to partially release in cellulose fibril distortion that (1) alters intra-chain hydrogen bonding and (2) then reduces the relative surface area to volume ratio of a cellulose fibril and subsequently increase the LFD (Hult et al. 2001; Foston and Ragauskas 2010). Increases in LFAD, as a result of pretreatment, are attributed to thermal induced crystallization and aggregate growth (Foston and Ragauskas 2010). The significant LFAD increases in acidic and organo-solv pretreated samples could be attributed to the removal and disruption of hemicellulose and lignin that obstruct cellulose co-crystallization (Oksanen et al.1997).

In addition, chemical reagents employed in the cellulose isolation process influence the cellulose structure to some extent (Xu et al. 2009; Ishizawa et al. 2009; Hubbell and Ragauskas 2010). However, the impact of isolation procedure on cellulose crystallinity and ultrastructure is minimal compared with those intensive hydrothermal pretreatments (Langan et al. 2014; Kumar et al. 2013).

Crystallite size analysis by WAXD

A complementary technique to evaluate cellulose microfibril ultrastructure is WAXD. This method is sensitive to the regular or repetitive arrangement of the atoms which is more commonly used to extract crystallite dimension information in cellulose samples with high precision (Park et al. 2010; Ibbett et al. 2013). Therefore, crystallite size was used to monitor cellulose fibril dimension change as a result of various pretreatments in this study.

As shown in Table 3, all pretreatment methods increase the size of the cellulose crystallite and the degree of that increase seems to depend again on pretreatment severity (encompassing pretreatment temperature, residence time, and method employed). The WAXD cellulose crystallite results show a similar trend or ordering with NMR LFD results (Table 2). Among the pretreatments, all acidic treatments have a large influence on cellulose microfibril structure, displaying a large increase in the crystallite size.

Table 3 Crystallite size (L200) for different pretreatment methods

Treatments	L200 ± 0.1 (nm) 5 min	L200 ± 0.1 (nm) 10 min	L200 ± 0.1 (nm) 60 min
Untreated	2.7	2.7	2.7
Hot water	3.0	3.3	4.0
Dilute acid	3.8	4.3	5.0
Dilute acid/Ox	4.1	4.1	4.5
Organo-solv	4.0	4.1	4.4
Lime[a]	3.8	–	4.1
Lime/Ox	3.6	3.6	3.6

[a] 10 min data not collected

WAXD studies have shown that irrespective of the kind of pretreatment applied such as alkaline, organic or acidic, the crystalline dimension of cellulose microfibrils increase within 5 min of pretreatment time. Hot water pretreatment produces the least increase in the cellulose crystallite size from an untreated sample 2.7–3.0 nm while all the other pretreatments increase from 2.7 to ~4.0 nm. Beyond 5 min of pretreatment cellulose crystallite dimensions increase greater than 4.0 nm, with dilute acid producing the most increase to 5.0 nm. This is interesting because scattering studies of sliced intact poplar chips indicate cellulose fibril—cellulose fibril distance is ~4.0 nm (Langan et al. 2014) and any increase in the crystallite size beyond 4.0 nm implies neighboring fibril coalescence. Langan et al. (2014) suggest fibril coalescence is driven by expulsion of interstitial biopolymer or solvent. This coalescing trend is however absent for the crystallite dimensions determined for cellulose in hot water, lime/Ox, and lime pretreated poplar. In summary, alkali pretreatments do not affect the cellulose crystallite dimension. This mostly likely is related to the fact alkali pretreatments were conducted at less severe conditions, and that not enough energy has been provided to overcome a kinetic barrier preventing cellulose microfibril coalescence.

Recalcitrance and enzymatic sugar release

Figure 5 summarizes the relative increase in glucose yield after enzymatic hydrolysis for the different pretreatments with respect to the untreated sample. In order of performance, the hot-water pretreatment displayed the lowest increase in glucose yield after enzymatic hydrolysis, dilute acid and dilute acid-oxidant pretreatments, which displayed very similar sugar release profiles were next, with the lime and lime-oxidant pretreatments producing slightly higher increase, and lastly the organo-solv pretreatment generated the largest increase in sugar yield.

Enzymatic hydrolysis of cellulosic biomass depends on several comprehensive factors including cell wall biopolymer distribution and chemistry, cellulose degree of polymerization and crystallinity, microfibril crystallite size and morphology, cell wall pore size and enzyme accessibility (Ding et al. 2012; Foston and Ragauskas 2010, 2012; Meng et al. 2013; Pu et al. 2006; Arantes and Saddler 2010). It has been postulated that crystalline regions reduce the resulting enzymatic degradation of cellulose (Hall et al. 2010), yet the cellulose crystallinity in most pretreated samples are greater than the untreated sample (Fig. 4). Accordingly, the literature clearly shows enzymatic saccharification of biomass which has undergone many of the pretreatments in this study, increase sugar yields suggesting cellulose crystallinity alone may not be the global determinant in the enzymatic degradability of pretreated biomass as once thought (Foston et al. 2011). Though true, when crystallinity is considered as a major factor, simple thermodynamic analysis suggests amorphous cellulose is more easily deconstructed than crystalline cellulose (Beguin and Aubert 1994; Hall et al. 2010). Therefore, minimizing cellulose crystallinity increase during thermochemical pretreatment may display superior sugar release profiles. In addition, various cellulose crystalline allomorphic states may respond differently to enzymatic hydrolysis. The metastable triclinic cellulose I_α is more susceptible to enzymatic hydrolysis (Pu et al. 2006; Boisset et al. 2000) and can be transformed into more stable monoclinic I_β by thermal treatment (Debzi et al. 1991; Foston and Ragauskas 2010). Large number of intra-chain hydrogen bonds in cellulose I_β with the increasing LFD is likely to present a thermodynamic barrier to the formation of a catalytically active complex with cellulases, which reduces enzymatic hydrolysis efficiency (Chundawat et al. 2011). Moreover, since the *para*-crystalline cellulose is believed to be located on the surface of crystallites as thin mono-cellular layers, which weaken the crystallites, increase cellulose dissolution and accessibility to reagents, and lead to

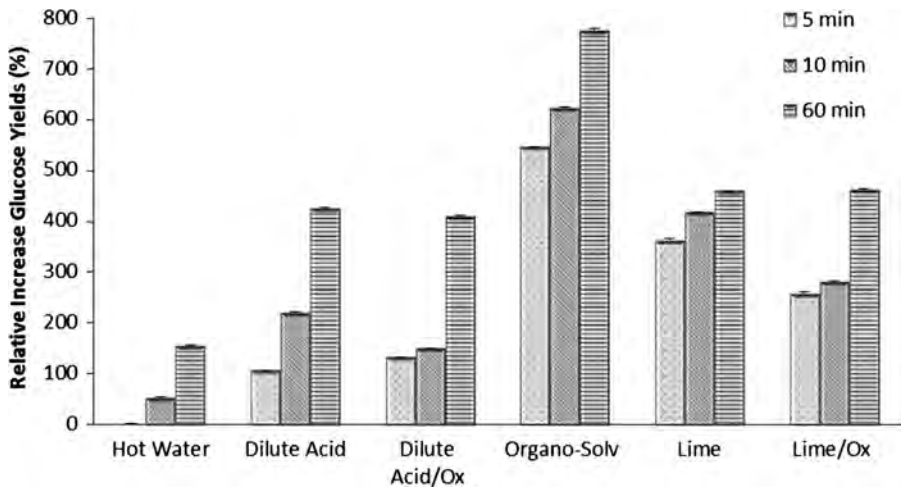

Fig. 5 The relative increase in glucose yields due to enzymatic hydrolysis of pretreated hybrid poplar solids with respect to the sugar release profile of the untreated solids

intra-lattice swelling (Ioelovich et al. 2010), therefore the increase of *para*-crystalline portion could also enhance the sugar yield in enzymatic hydrolysis.

Conclusions

In particular, key molecular features related to biomass recalcitrance, specifically cellulose ultrastructure, were studied. There is no a large influence of those pretreatments on cellulose crystallinity. However, compared with lime and lime/Ox pretreatments, acidic pretreatments relatively significantly alter cellulose ultrastructure, increasing cellulose % crystallinity and cellulose crystallite size significantly. The extent of these changes to cellulose ultrastructure seems to be related to pretreatment severity (time, temperature, and pH), suggesting the kinetics of (1) microfibril coalescence, (2) cellulose crystalline transformation, (3) xylan/lignin removal/redistribution, and (4) selective cellulose component degradation determine the type and the extent of changes that occurs to cellulose ultrastructure during pretreatment. Lignin removal during alkaline and organo-solv pretreatments is a key factor in enhancing the sugar yield. Moreover, the large increase of LFD, crystallite size, and *para*-crystalline cellulose in organo-solv pretreatment along with high sugar yield seems to suggest the increased proportion of *para*-crystalline cellulose could also be beneficial to enhance the sugar yield in enzymatic hydrolysis.

A direct correlation between these measured molecular features and reduced biomass recalcitrance cannot be made because of the numerous other inter-related substrate characteristics being modified during pretreatment. However, as shown in this study, clear changes in cellulose ultrastructure do occur, many of which could be tailored or optimized by the choice of pretreatment and pretreatment conditions.

Acknowledgments Hybrid poplar samples were obtained through a collaborative agreement with the Bioenergy Science Center (BESC) located at the Oak Ridge National Laboratory, Oak Ridge, Tennessee. This research is funded by the Genomic Science Program, Office of Biological and Environmental Research, U. S. Department of Energy, under FWP ERKP752 and US Department of Energy sponsored BioEnergy Science Center (BESC). Oak Ridge National Laboratory's Center for Structural Molecular Biology (CSMB) is supported by the Office of Biological and Environmental Research (FWP ERKP291). A portion of this research was also conducted at the Center for Nanophase Materials Sciences, which is sponsored at Oak Ridge National Laboratory by the Scientific User Facilities Division, Office of Basic Energy Sciences, U. S. Department of Energy. Q. S. is grateful for the financial support from the Paper Science & Engineering (PSE) fellowship program at Institute of Paper Science & Technology (IPST) at Georgia Institute of Technology.

References

Arantes V, Saddler JN (2010) Access to cellulose limits the efficiency of enzymatic hydrolysis: the role of amorphogenesis. Biotechnol Biofuels 3

Beguin P, Aubert JP (1994) The biological degradation of cellulose. FEMS Microbiol Rev 13:25–58

Boisset C, Fraschini C, Schulein M, Henrissat B, Chanzy H (2000) Imaging the enzymatic digestion of bacterial cellulose ribbons reveals the endo character of the cellobiohydrolase Cel6A from Humicola insolens and its mode of synergy with cellobiohydrolase Cel7A. Appl Environ Microbiol 66:1444–1452

Brosse N, Sannigrahi P, Ragauskas A (2009) Pretreatment of *Miscanthus x giganteus* using the ethanol organosolv process for ethanol production. Ind Eng Chem Res 48:8328–8334

Brunner AM, Busov VB, Strauss SH (2004) Poplar genome sequence: functional genomics in an ecologically dominant plant species. Trends Plant Sci 9:49–56

Bubner P, Plank H, Nidetzky B (2013) Visualizing cellulase activity. Biotechnol Bioeng 110:1529–1549

Chang VS, Burr B, Holtzapple MT (1997) Lime pretreatment of switchgrass. Appl Biochem Biotechnol 63–5:3–19

Chang VS, Nagwani M, Holtzapple MT (1998) Lime pretreatment of crop residues bagasse and wheat straw. Appl Biochem Biotechnol 74:135–159

Chang VS, Nagwani M, Kim CH, Holtzapple MT (2001) Oxidative lime pretreatment of high-lignin biomass—poplar wood and newspaper. Appl Biochem Biotechnol 94:1–28

Chen YM, Wang Y, Wan JQ, Ma YW (2010) Crystal and pore structure of wheat straw cellulose fiber during recycling. Cellulose 17:329–338

Chundawat SPS, Bellesia G, Uppugundla N, Sousa LD, Gao DH et al (2011) Restructuring the crystalline cellulose hydrogen bond network enhances its depolymerization rate. J Am Chem Soc 133:11163–11174

Cullity BD, Stock SR (2001) Elements of X-ray diffraction, 3rd edn. Prentice Hall, Upper Saddle River

Davis MW (1998) A rapid modified method for compositional carbohydrate analysis of lignocellulosics by high pH anion exchange chromatography with pulsed amperometric detection (HPAEC/PAD). J Wood Chem Technol 18: 235–252

Debzi EM, Chanzy H, Sugiyama J, Tekely P, Excoffier G (1991) The Iα → Iβ transformation of highly crystalline cellulose by annealing in various mediums. Macromolecules 24:6816–6822

Ding SY, Liu YS, Zeng YN, Himmel ME, Baker JO, Bayer EA (2012) How does plant cell wall nanoscale architecture correlate with enzymatic digestibility? Science 338:1055–1060

Diniz J, Gil MH, Castro J (2004) Hornification—its origin and interpretation in wood pulps. Wood Sci Technol 37: 489–494

Foston M, Ragauskas AJ (2010) Changes in lignocellulosic supramolecular and ultrastructure during dilute acid pretreatment of *Populus* and switchgrass. Biomass Bioenergy 34:1885–1895

Foston M, Ragauskas AJ (2012) Biomass characterization: recent progress in understanding biomass recalcitrance. Ind Biotechnol 8:191–208

Foston M, Hubbell CA, Davis M, Ragauskas AJ (2009) Variations in cellulosic ultrastructure of poplar. Bioenergy Res 2:193–197

Foston M, Hubbell CA, Samuel R, Jung S, Fan H, Ding SY, Zeng YN, Jawdy S, Davis M, Sykes R, Gjersing E, Tuskan GA, Kalluri U, Ragauskas AJ (2011) Chemical, ultrastructural and supramolecular analysis of tension wood in *Populus tremula x alba* as a model substrate for reduced recalcitrance. Energy Environ Sci 4:4962–4971

Hall M, Bansal P, Lee JH, Realff MJ, Bommarius AS (2010) Cellulose crystallinity—a key predictor of the enzymatic hydrolysis rate. FEBS J 277:1571–1582

Hu F, Ragauskas AJ (2012) Pretreatment and lignocellulosic chemistry. Bioenergy Res 5:1043–1066

Hubbell CA, Ragauskas AJ (2010) Effect of acid-chlorite delignification on cellulose degree of polymerization. Bioresour Technol 101:7410–7415

Hult EL, Larsson PT, Iversen T (2001) Cellulose fibril aggregation—an inherent property of kraft pulps. Polymer 42:3309–3314

Ibbett R, Gaddipati S, Hill S, Tucker G (2013) Structural reorganisation of cellulose fibrils in hydrothermally deconstructed lignocellulosic biomass and relationships with enzyme digestibility. Biotechnol Biofuels 6:33

Ioelovich M, Leykin A, Figovsky O (2010) Study of cellulose paracrystallinity. BioResources 5:1393–1407

Ishizawa CI, Jeoh T, Adney WS, Himmel ME, Johnson DK, Davis MF (2009) Can delignification decrease cellulose digestibility in acid pretreated corn stover? Cellulose 16:677–686

Klug HP, Alexander LE (1974) X-ray diffraction procedures for polycrystalline and amorphous materials, 2nd edn. Wiley, New York

Kumar R, Mago G, Balan V, Wyman CE (2009) Physical and chemical characterizations of corn stover and poplar solids resulting from leading pretreatment technologies. Bioresour Technol 100:3948–3962

Kumar R, Hu F, Hubbell CA, Ragauskas AJ, Wyman CE (2013) Comparison of laboratory delignification methods, their selectivity, and impacts on physiochemical characteristics of cellulosic biomass. Bioresour Technol 130:372–381

Langan P et al (2014) Common processes drive the thermochemical pretreatment of lignocellulosic biomass. Green Chem 16:63–68

Lloyd TA, Wyman CE (2005) Combined sugar yields for dilute sulfuric acid pretreatment of corn stover followed by enzymatic hydrolysis of the remaining solids. Bioresour Technol 96:1967–1977

Maciel GE, Kolodziejski WL, Bertran MS, Dale BE (1982) Carbon-13 NMR and order in cellulose. Macromolecules 15:686–687

Martin C, Klinke HB, Thomsen AB (2007) Wet oxidation as a pretreatment method for enhancing the enzymatic convertibility of sugarcane bagasse. Enzyme Microb Technol 40:426–432

Meng X, Foston M, Leisen J, DeMartini J, Wyman CE, Ragauskas AJ (2013) Determination of porosity of lignocellulosic biomass before and after pretreatment by using Simons' stain and NMR techniques. Bioresour Technol 144:467–476

Mosier N, Hendrickson R, Ho N, Sedlak M, Ladisch MR (2005a) Optimization of pH controlled liquid hot water pretreatment of corn stover. Bioresour Technol 96:1986–1993

Mosier N, Wyman C, Dale B, Elander R, Lee YY, Holtzapple M, Ladisch M (2005b) Features of promising technologies for pretreatment of lignocellulosic biomass. Bioresour Technol 96:673–686

Newman RH (2004) Carbon-13 NMR evidence for cocrystallization of cellulose as a mechanism for hornification of bleached kraft pulp. Cellulose 11:45–52

Oksanen T, Buchert J, Viikari L (1997) The role of hemicelluloses in the hornification of bleached kraft pulps. Holzforschung 51:355–360

Ostlund A, Kohnke T, Nordstierna L, Nyden M (2010) NMR cryoporometry to study the fiber wall structure and the effect of drying. Cellulose 17:321–328

Pan XJ, Xie D, Yu RW, Saddler JN (2008) The bioconversion of mountain pine beetle-killed lodgepole pine to fuel ethanol using the organosolv process. Biotechnol Bioeng 101: 39–48

Park S, Baker JO, Himmel ME, Parilla PA, Johnson DK (2010) Cellulose crystallinity index: measurement techniques and their impact on interpreting cellulose performance. Biotechnol Biofuels 3:10

Pu Y, Ziemer C, Ragauskas AJ (2006) CP/MAS C-13 NMR analysis of cellulase treated bleached softwood kraft pulp. Carbohydr Res 341:591–597

Samuel R, Pu Y, Foston M, Ragauskas AJ (2010) Solid-state NMR characterization of switchgrass cellulose after dilute acid pretreatment. Biofuels 1:85–90

Sannigrahi P, Miller SJ, Ragauskas AJ (2010a) Effects of organosolv pretreatment and enzymatic hydrolysis on cellulose structure and crystallinity in loblolly pine. Carbohydr Res 345:965–970

Sannigrahi P, Ragauskas AJ, Miller SJ (2010b) Lignin structural modifications resulting from ethanol organosolv treatment of loblolly pine. Energy Fuels 24:683–689

Sannigrahi P, Ragauskas AJ, Tuskan GA (2010c) Poplar as a feedstock for biofuels: a review of compositional characteristics. Biofuels Bioprod Biorefining 4:209–226

Sannigrahi P, Kim DH, Jung S, Ragauskas AJ (2011) Pseudo-lignin and pretreatment chemistry. Energy Environ Sci 4:1306–1310

Studer MH, DeMartini JD, Brethauer S, McKenzie HL, Wyman CE (2010) Engineering of a high-throughput screening system to identify cellulosic biomass, pretreatments, and enzyme formulations that enhance sugar release. Biotechnol Bioeng 105:231–238

Sturcova A, His I, Apperley DC, Sugiyama J, Jarvis MC (2004) Structural details of crystalline cellulose from higher plants. Biomacromolecules 5:1333–1339

VanderHart DL, Atalla RH (1984) Studies of microstructure of native celluloses using solid-state 13 C NMR. Macromolecules 17:1465–1472

Wang ZY, Cheng JJ (2011) Lime pretreatment of coastal bermudagrass for bioethanol production. Energy Fuels 25:1830–1836

Wickholm K, Larsson PT, Iversen T (1998) Assignment of non-crystalline forms in cellulose I by CP/MAS 13C NMR spectroscopy. Carbohydr Res 312:123–129

Wyman CE, Dale BE, Elander RT, Holtzapple M, Ladisch MR, Lee YY, Mitchinson C, Saddler JN (2009) Comparative sugar recovery and fermentation data following pretreatment of poplar wood by leading technologies. Biotechnol Prog 25:333–339

Xu JL, Cheng JJ (2011) Pretreatment of switchgrass for sugar production with the combination of sodium hydroxide and lime. Bioresour Technol 102:3861–3868

Xu F, Ding H, Tejirian A (2009) Detrimental effect of cellulose oxidation on cellulose hydrolysis by cellulase. Enzyme Microb Technol 45:203–209

Xu JL, Cheng JJ, Sharma-Shivappa RR, Burns JC (2010) Lime pretreatment of switchgrass at mild temperatures for ethanol production. Bioresour Technol 101:2900–2903

Zhao HB, Kwak JH, Wang Y, Franz JA, White JM, Holladay JE (2006) Effects of crystallinity on dilute acid hydrolysis of cellulose by cellulose ball-milling study. Energy Fuels 20:807–811